Energy 240 (2022) 122810

Contents lists available at ScienceDirect

Energy

journal homepage: www.elsevier.com/locate/energy

Optimal recovery of thermal energy in liquid air energy storage

Zhongxuan Liu [a], Donghoi Kim [b], Truls Gundersen [a, *]

[a] Department of Energy and Process Engineering, Norwegian University of Science and Technology, Kolbjoern Hejes vei 1A, NO-7491, Trondheim, Norway
[b] SINTEF Energy Research, Sem Sælands vei 11, NO-7465, Trondheim, Norway

ARTICLE INFO

Article history:
Received 5 January 2021
Received in revised form
1 December 2021
Accepted 2 December 2021
Available online 6 December 2021

Keywords:
Liquid air energy storage
Round-trip efficiency
Cold energy recovery cycle
Particle swarm optimization

ABSTRACT

The increasing share of renewables in energy systems requires energy storage technologies to handle intermittent energy sources and varying energy sinks. Liquid air energy storage (LAES) is a promising technology since it has a high energy density and is not geographically constrained. A relatively high round-trip efficiency (RTE) is obtained by using hot and cold energy recovery cycles in the LAES. In this work, seven cases related to different cold energy recovery cycles are optimized and compared for a standalone LAES system. Multi-component fluid cycles (MCFCs) and Organic Rankine Cycles (ORCs) are considered for the first time to be used as cold recovery cycles in the LAES. The optimal results show that the LAES system with dual MCFC has the best performance with an RTE of 62.4%. This RTE can be further increased to 64.7% by reducing the minimum temperature difference of high-temperature heat exchangers from 10 °C to 5 °C. Optimization results also indicate that ORCs used in the cold energy recovery system are not producing any work, and only phase change of the working fluid takes place, thus they should not be used. Finally, the exergy transfer effectiveness is applied to measure thermodynamic performance of the charging and discharging processes.

1. Introduction

Currently, energy systems are still dominated by fossil fuels. More than 80% of world energy consumption comes from coal, oil and natural gas [1]. However, these energy forms will be partly replaced in the future to mitigate world average temperature increase due to greenhouse gas emissions. The proportion of renewables in energy systems has grown steadily over the last decade to 5.7% in 2020. British Petroleum predicts that the primary energy consumption based on fossil fuels will drop from approximately 85% in 2018 to below 70% by 2050, and the share of renewable energy will be growing to at least 20% in 2050 [2]. As more renewable energy enters the energy market, one major issue is related to the fact that the stability of energy markets will be threatened due to the intermittency of the most frequently used new renewable energies, e.g. wind and solar energy. Such irregular and unstable renewable energies cannot ensure a stable supply to meet demands from end users. Moreover, a lot of renewable power will be wasted in periods when the production exceeds the demand. The use of energy storage technologies could balance the renewable power supply and the grid demand and thereby increase the effective utilization of renewable energy. Energy storage technologies are able to store any surplus power generated from renewable energies and provide energy in different forms according to user needs [3].

Energy storage technologies can also be applied in distributed energy systems (DES). In DES, unlike traditional large-scale power plants, the large energy conversion units are substituted by smaller ones, which are easier to locate close to end users. The DES is a new trend for energy systems. The objective of a DES is to make full and effective use of local resources [4]. A small-scale power plant is flexible and can be built based on the available resources. It can also be integrated with other power plants when local needs cannot be met. Thus, the DES, which is a network of energy hubs, is able to replace traditional power plants in terms of energy demand. In addition, a DES can employ various energy conversion technologies, using different energy sources (such as renewable energies), and provide different forms of energy (such as heat and power). Energy storage technologies are important in such systems since they can ensure the transition from traditional centralized systems to decentralized energy systems where renewable energy can be involved without limitations.

The most mature electrical energy storage (EES) technologies are batteries [5], pumped hydroelectric energy storage (PHES) [6],

* Corresponding author.
E-mail address: truls.gundersen@ntnu.no (T. Gundersen).

https://doi.org/10.1016/j.energy.2021.122810

and compressed air energy storage (CAES) [7]. However, the application of these technologies is limited by their drawbacks. Batteries are scarcely used in industrial systems since large-scale batteries have high maintenance costs and short life cycles. PHES and CAES can be used for large-scale energy storage, but they can only be applied in certain cases because of their geographical constraints. The working fluids for these two technologies are water and air, which have low energy densities so that large storage volumes are required for PHES and CAES. Actually, reservoirs at different elevations are adopted to store water in PHES, while underground caverns and expensive high-pressure tanks are used to store compressed air in CAES. Thus, an EES technology that can overcome the drawbacks of these technologies is needed to promote the development and application of EES. This means, among other considerations, that it can be easily located where excess energy is available.

Among various proposals, liquid air energy storage (LAES) has been suggested to have outstanding performance compared with the mentioned energy storage technologies [8,9]. Energy is stored in liquid air with a higher energy density, so the volume of storage tanks is considerably reduced. The use of LAES also avoids the geographical constraints of PHES and CAES. In addition, the LAES can be integrated with other energy conversion processes, and it can be located near these processes to avoid additional pipelines and corresponding costs. Thus, the LAES is a promising alternative for large-scale energy storage.

The first reported application of liquid air as a working fluid for energy storage refers to Newcastle in 1977 [10]. A regenerator was adopted to collect the compression heat from high temperature air (800 °C) and release it to the air expansion part. The recovery ratio is claimed to be 62%, and it is improved to 72% with additional fuel combustion. The largest existing LAES, that has been in operation in the UK since 2018 [11], has a storage capacity of 15 MWh (54 GJ). A round-trip efficiency (RTE) of 60% has been reached for this standalone LAES. The recovery ratio, which is another term used for round-trip efficiency, quantifies the amount of energy that is recovered from various storage technologies. The RTE is commonly applied in EES to evaluate different technologies. In order to increase the competitiveness of the LAES, various methods have been used to improve the overall performance of the process.

Guizzi et al. [12] studied an LAES system that utilizes storages of heat from adiabatic compression and cold duty from regasification. An RTE of 54.4% was obtained with effective hot and cold thermal energy recirculation between the charging and discharging processes. Morgan et al. [13] tried to improve the efficiency of the LAES system by adding a Claude cycle to the low-temperature heat exchanger. The air was further cooled down before entering the separator. As a result, the RTE was improved to 57%. Borri et al. [14] simulated and compared three microgrid scale LAES systems with different liquefaction cycles, i.e. the Linde, Claude and Kapitza cycles. The optimal configuration of the liquefaction part was the Kapitza cycle with two-stage compression and the specific energy consumption can be reduced by up to 25% by optimizing the operating conditions (recirculation ratio and flash pressure). Liu et al. [15] investigated the effect of different number of compression and expansion stages on the system efficiency of the LAES system. The temperature and flow rate of the thermal oil will change with different number of compression stages. Accordingly, pinch points in reheaters and the inlet air temperature to expanders in the discharging process will vary due to changes in the hot thermal energy storage. Results show that the LAES system with a 2-stage compressor and a 3-stage expander has an RTE of 58.2%, which is higher than other configurations. Chen et al. [16] considered phase change materials (PCMs) as the cold storage fluid between the charging and discharging processes in the LAES system. It is found that the optimal design of the cold storage process consists of 12 stages with 12 different PCMs, which means that one type of PCM is used at each stage that is operated at a certain temperature. The RTE of the LAES system with the optimal cold storage process is 54.2%. Peng et al. [17] found that about 20–45% of the compression heat in the LAES was not used in the discharging process. To further increase the performance of the system, an ORC and an ORC-Absorption Refrigeration Cycle were proposed and embedded in the LAES. A higher RTE of 62.7% was obtained with the LAES-ORC system, which has a simpler layout.

The aforementioned studies focus on the improvement of a standalone LAES system. In addition, the integration of the LAES system with other processes to enhance the performance of the LAES has also been considered. Li et al. [18] studied the integration of an LAES with a nuclear power plant (NPP) to utilize the excess reaction heat. This further increased the inlet air temperature to expanders, and an RTE of 71.3% could be reached. Cetin et al. [19] tried to use a geothermal power plant to drive an LAES system. The power generated from the geothermal plant supports air liquefaction in the LAES, and the waste geothermal heat was used to increase the inlet air temperature to expanders in the discharging process. The RTE of the LAES was 46.7%, while the thermal efficiency of the combined system was increased from 6.6 to 24.4% when the geothermal heat was supplied at 180 °C. Lee et al. [20] integrated the LAES with liquefied natural gas (LNG). Cold energy from LNG regasification is collected and used to liquefy air in the LAES, and power is generated from the expansion of both natural gas and air. The performance of the charging and discharging parts has been improved, and the corresponding exergy efficiencies are 94.2% and 61.1%. Lee and You [21] performed a similar study, where air was liquified by obtaining the cold thermal energy from LNG regasification. In this case, direct expansion was used for the power generation from LNG and liquid air, and an Organic Rankine Cycle (ORC) with a multi-component working fluid was applied to produce additional power in LNG regasification before the NG expansion part. The exergy efficiency of the combined process was 70.3%. Qi et al. [22] further improved the combined system with the LAES and an LNG regasification process. During discharging, both the LAES discharging process and the LNG regasification process are used to produce power. During charging, the LNG is first used to cool the charging process in LAES, and then it is fed to an ORC to utilize the remaining cold energy. The RTE of the combined system reaches 129.2%, since the cold energy from LNG is regarded as “free” and would otherwise be lost. Antonelli et al. [23] analyzed and compared different configurations of the discharging process in the LAES: direct expansion, direct expansion combined with additional combustion heat, and direct expansion combined with both additional combustion heat and an ORC or a Brayton Cycle. Results demonstrated that the LAES with additional combustion heat and a Brayton Cycle (the last case) has the highest RTE of 90%.

A comparison of system performance (RTE) between the abovementioned publications is summarized in Table 1. As the table clearly indicates, the performance can be significantly improved by integrating the LAES system with external hot or cold thermal energy sources. For a standalone system, the RTE of the LAES is increased considerably with the use of hot and cold thermal energy storages. In the hot storage cycle, the working fluid is thermal oil that is first used to collect the compression heat from the charging process, and then used to release the heat to the expansion part of the discharging process. The temperature difference between the thermal oil (cold stream) and the compressed air (hot stream) is evenly distributed within the temperature range of the compression heat exchanger, since no phase change takes place. For cold energy recovery and storage systems that consist of two pure working fluid cycles (i.e. methanol and propane), the situation is

Table 1
A comparison between recent LAES publications.

References	System type	Integrated process	Additional cycle	Round-trip efficiency (%)
Smith [10]	Standalone			62.0
Highview power [11]	Standalone			60.0
Guizzi et al. [12]	Standalone			54.4
Morgan et al. [13]	Standalone			57.0
Liu et al. [15]	Standalone			58.2
Chen et al. [16]	Standalone			54.2
Peng et al. [17]	Standalone		ORC	62.7
Li et al. [18]	Integrated	Nuclear power		71.3
Cetin et al. [19]	Integrated	Geothermal power		46.7
Lee et al. [20]	Integrated	LNG regasification		172.1
Lee and You [21]	Integrated	LNG regasification	ORC	122.8
Qi et al. [22]	Integrated	LNG regasification	ORC	129.2
Antonelli et al. [23]	Integrated	Combustion	Brayton	90.0

different. The cold storage cycles are used to transfer the cold thermal energy from the regasification of liquid air in the discharging process to the air liquefaction part in the charging process. The operating pressure for air liquefaction is usually larger than the critical pressure of air (37.8 bar) to avoid phase change at constant temperature (a horizontal line in the composite curves for the heat exchanger), so that a smooth liquefaction curve is obtained with decreasing temperature. This makes it easier to find a working fluid to match with the liquefaction curve of air. The methanol and propane cycles in the system have acceptable performances (they both operate in liquid form, so only sensible heat is involved), but they still contribute to considerable exergy losses in the LAES related to irreversibilities caused by large temperature differences in the heat exchangers.

Based on the observations above, it is clear that the research on standalone LAES systems is far from complete. There is a lack of research on studying alternative fluids for cold energy storage cycles in the LAES system, such as multi-component fluid cycles (MCFCs). The MCFC can provide a wider range of temperature profiles than single-component fluid cycles, and a better match between hot and cold composite curves is obtained. Organic Rankine Cycles offer another solution for cold storage cycles. ORCs can produce electricity by utilizing the temperature difference between the air regasification and liquefaction. At the same time, it is used to transfer the cold duty from air regasification to liquefaction. The working fluid for the ORC is multi-component, so the heating and cooling curves of the working fluid are closer to the temperature profile of the air, and the performance of the LAES will be improved with reduced exergy losses in the cold box. In addition, in the available literature, neither deterministic methods nor stochastic search have been applied to optimize the LAES process with respect to specific power consumption or round-trip efficiency.

Thus, in this study, multi-component fluid cycles and Organic Rankine Cycles are used for the first time to transfer the cold thermal energy of regasification to the liquefaction of air in the LAES system. A particle swarm optimization (PSO) method is adopted to find the optimal composition of the multi-component fluids [24]. Cases related to LAES systems with different storage cycles for cold thermal energy recovery are simulated, optimized and compared in Section 5.

2. System description

The flowsheet of the liquid air energy storage with hot and cold storage cycles is shown in Fig. 1. The LAES system consists of three parts: charging, storage, and discharging. In the charging part, air is first compressed in a four-stage compressor with inter/aftercoolers (air is cooled to 30 °C after each compression stage), then it is cooled by heat exchangers in the cold box, before being expanded to atmospheric pressure in a cryo-turbine, which is used to generate refrigeration capacity and power. The liquid fraction is sent to storage, while the vapor fraction is recirculated to the compression section. The charging process is essentially a liquefaction process, where air is liquefied in periods with excess electric power. In other words, energy (or power) is stored in the form of liquid air. In the storage part, liquid air is kept in atmospheric cryogenic tanks. In the discharging part, liquid air is pumped to a higher pressure before being regasified in evaporators by receiving heat from the cold storage fluids. High-pressure air is then fed to a 4-stage turbine to generate electricity. In order to improve the performance of the LAES system, hot and cold thermal energy storages are employed. The compression heat is used to increase the temperature of inlet air to the expansion stages and thereby produce more electricity in the discharging process. Thermal oil is used as working fluid in the hot thermal energy storage cycle. The cold thermal energy from air regasification is stored in cold intermediate fluids and will be released to the air liquefaction part.

In this study, the LAES system with methanol and propane cycles for cold energy recovery is regarded as the Base Case (see Fig. 2). Other cases related to different cold thermal energy recovery cycles for the LAES system are considered. To simplify the system, one multi-component fluid cycle (Case 1) is considered to replace the two single-component cycles in the Base Case. Two multi-component fluid cycles are also evaluated for the cold energy recovery system (Case 2). As mentioned before, ORCs could provide extra power while transferring the cold duty from the discharging to the charging process. A single ORC is considered as the cold energy recovery cycle in Case 3. Different combinations of an ORC and a single component fluid cycle are used as the cold energy recovery system as well. An ORC and a propane cycle are considered in Case 4, while a methanol cycle and an ORC are used in Case 5. Two ORCs are also evaluated as cold energy recovery cycles in Case 6. The components in the working fluids for cold energy recovery cycles are nitrogen, methane, methanol, ethane, propane and n-butane. Although somewhat arbitrarily, the reason for selecting these components is that they can cover the temperature ranges of air liquefaction and regasification (the boiling points and freezing points of these components are considered). In addition, the isobaric specific heat capacities of these six components are close to the specific heat capacity of air for relevant pressure conditions.

2.1. Multi-component fluid cycles for cold recovery

The purpose of the fluids in the cold energy storage is to transfer cold thermal energy from air regasification to the air liquefaction part. Actually, in LAES systems, the charging and discharging

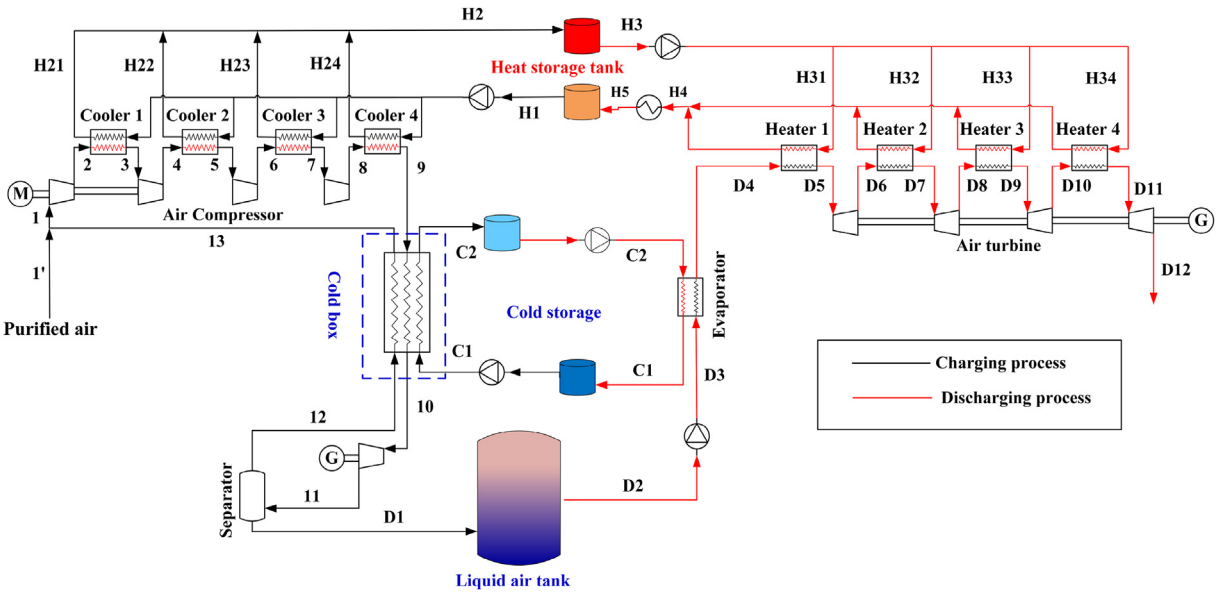

Fig. 1. Flow diagram for the liquid air energy storage (LAES).

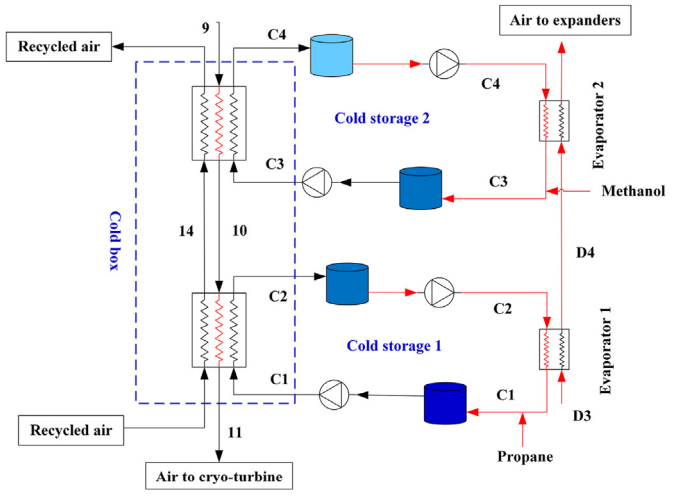

Fig. 2. Methanol and propane cycles [10] for cold energy recovery in the LAES – Base case.

processes typically do not operate at the same time. When energy is demanded, the discharging process is in operation and provides cold regasification energy to fluids from the high-temperature storage tanks. The fluids cooled by the discharging process are then stored in low-temperature storage tanks. When excess electricity is available, the fluids that carry the cold regasification energy are made available for the charging process to provide refrigeration capacity to liquefy air. After receiving heat from the air, the fluids are stored in high-temperature storage tanks to complete the cycle.

A major limitation with single component working fluids is that their operating range for temperature cannot meet the requirements of the entire temperature span in the system. Thus, if the cooling task of hot streams is to be carried out along a wider temperature range, either the fluid needs to go through a phase change, or additional fluid cycles must be used to avoid phase changes. In the former case, a single component cold fluid experiences a constant temperature during phase change, which results in considerable exergy losses and thereby poor thermodynamic performance. In the latter case, extra cycles in the LAES will increase the complexity and cost. Multi-component fluids, unlike pure components, can customize the composition and thereby make the operating temperature range wider while considering the freezing and boiling points of the components. A good match between the temperature profiles of hot and cold streams can be obtained while keeping the configuration simple when using multi-component fluids.

Generally, liquids always have better performance than gases in terms of transferring heat, so the cold storage fluids should remain in liquid phase throughout the LAES system. In this section, two different configurations of cold storage cycles that use different components are illustrated in Fig. 3. Fig. 3a shows a single multi-component cycle (Case 1) that contains nitrogen, methane, ethane and propane. Fig. 3b shows a dual multi-component fluid cycle (Case 2). Methane, ethane, propane and n-butane are used in the first cycle that is operating at higher temperature. In the second cycle, n-butane is changed to nitrogen since the freezing point of n-butane is −138 °C, which is much higher than the boiling point of air (−194 °C). Therefore, nitrogen, methane, ethane and propane are considered for the second cycle.

2.2. Organic Rankine Cycles for cold energy recovery

Organic Rankine Cycles are also considered for cold energy recovery. They can not only be used to transfer cold duty from the discharging to the charging process, but also to generate additional power due to the temperature difference between the air liquefaction and regasification. Any power produced by the cold energy recovery cycles is expected to improve the RTE. However, the specific enthalpy of the working fluid is reduced after being expanded through the gas turbine of the ORC (both temperature and pressure of the fluid are reduced), so the cold regasification energy collected by the same amount of working fluid decreases. This reduces the efficiency of the LAES system, since the temperature of the regasified air is decreased before air is entering the expansion section, resulting in reduced expansion work. The trade-off between the ORC power output and the reduced expansion work means there is an optimal operating condition for the ORC,

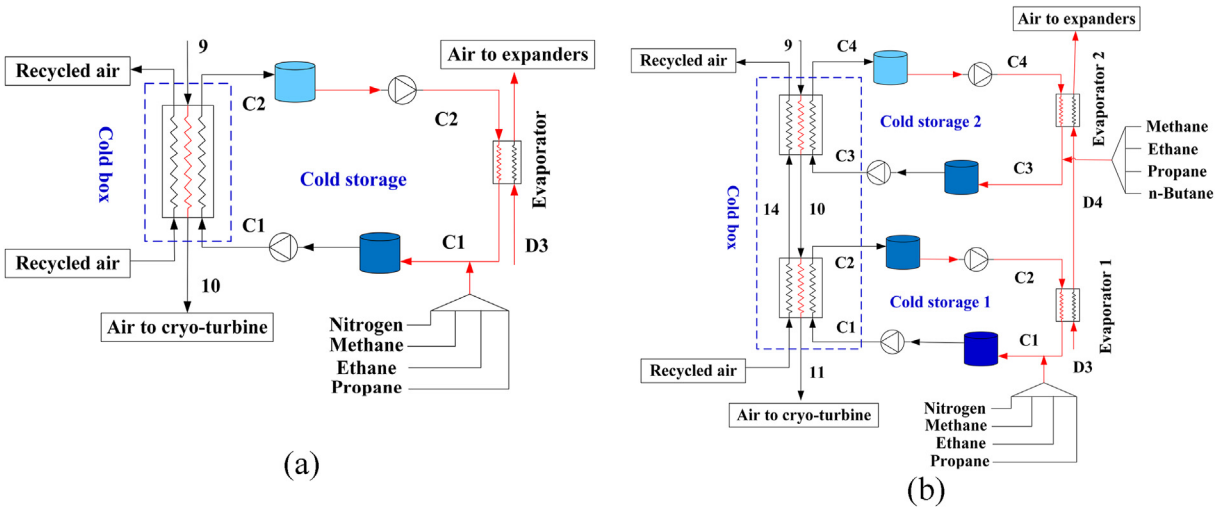

Fig. 3. Different layouts for cold storage cycles in the LAES system. a) Case 1 (Single multi-component fluid cycle); b) Case 2 (Dual multi-component fluid cycle).

which will be discussed in Section 5.1.

When electricity is required, ORC working fluids from high-temperature tanks are sent to the liquid air evaporator to collect the cold regasification energy from air during the phase change. After exchanging heat with evaporating air, the working fluids are stored in low-temperature tanks. When the charging process is in operation, working fluids are first pumped to high pressure before being sent to the cold box, where the working fluids are completely evaporated, and the high-pressure air is partly liquefied. In order to produce more electricity, the ORC working fluids enter the gas turbines, before being stored in high-temperature tanks to complete the cycles.

Four cases related to different combinations of ORCs and a single component fluid cycle are illustrated in Fig. 4. Fig. 4a shows a single ORC (Case 3) that contains nitrogen, methane, ethane and propane. Fig. 4b illustrates an ORC and a propane cycle (Case 4). The components of the ORC are ethane, propane and n-butane. Fig. 4c presents the combination of a methanol cycle and an ORC (Case 5). The components of the ORC are nitrogen, methane, ethane, and propane. In Fig. 4b (Case 4), the ORC operates at higher temperatures in the cold box while the propane cycle operates at lower temperatures. This is in contrast to Fig. 4c (Case 5), where the ORC operates at lower temperatures in the cold box while the methanol cycle operates at higher temperatures. Fig. 4d illustrates a dual ORC (Case 6). The components of the working fluid in the 1st ORC that is operated at a higher temperature are ethane, propane and n-butane, while the components of the working fluid in the 2nd ORC that is operated at a lower temperature are nitrogen, methane, ethane, and propane.

3. Process evaluation

Several Key Performance Indicators (KPIs) can be used to evaluate LAES systems, depending on the definition of system performance. In this work, the KPIs considered are liquid yield, round-trip efficiency, specific power consumption and exergy efficiency. Liquid yield, which is an important parameter for processes involving air liquefaction, is related to the liquid air fed to the discharging process and the part of air recycled to the charging process. A higher liquid yield leads to less compression work, since the recirculation ratio is reduced, and less air is re-compressed. The round-trip efficiency is a commonly used parameter in energy storage systems, including EES, to evaluate different technologies. It quantifies the amount of power that is recovered relative to the amount of power used to store the energy for different energy storage technologies. Specific power consumption indicates the efficiency of the charging process. Finally, exergy efficiency could also be considered for comparing different energy storage technologies. In this work, the exergy transfer effectiveness, which can evaluate the exergy transfer between the charging and the discharging processes, is used to measure exergy efficiency of the LAES system.

As will be shown in Section 5, despite their apparent differences, these four KPIs are related and they all address the energy performance of the system. Definitions of these KPIs are provided in the following.

The outlet stream of the LAES charging process is separated into a liquid and a vapor stream after precooling and expansion. The vapor stream leaving the separator is returned to the compressor train. This recycled stream inside the charging part of the LAES results in a larger amount of air flowing through the compressors compared to the liquid air from storage tanks. Thus, liquid yield is the ratio between the flow rate of liquid air to the discharging part and the total flow rate of air compressed in the charging part, and is calculated by Equation (1).

$$\eta_{LY} = \frac{\dot{m}_{liq}}{\dot{m}_{comp}} \tag{1}$$

Here, $\dot{m}_{liq}$ and $\dot{m}_{comp}$ represent the mass flow rates of liquid air and air entering the compressors, respectively.

The round-trip efficiency is defined as the work produced ($\dot{W}_{out}$) in the discharging process divided by the work consumed ($\dot{W}_{in}$) in the charging process, see Equation (2).

$$\eta_{RT} = \frac{\dot{W}_{out}}{\dot{W}_{in}} = \frac{\dot{m}_{liq} w_{tur}}{\dot{m}_{comp} w_{comp}} = \eta_{LY} \cdot \frac{w_{tur}}{w_{comp}} \tag{2}$$

Here, w_{comp} and w_{tur} denote the specific work of compressors in the charging process and turbines in the discharging process, respectively.

Specific power consumption (*SPC*), which is given by Equation (3), is the net work consumed per mass of liquid air produced.

$$SPC = \frac{\dot{W}_{net}}{\dot{m}_{liq}} \tag{3}$$

The net work ($\dot{W}_{net}$) required is calculated by Equation (4).

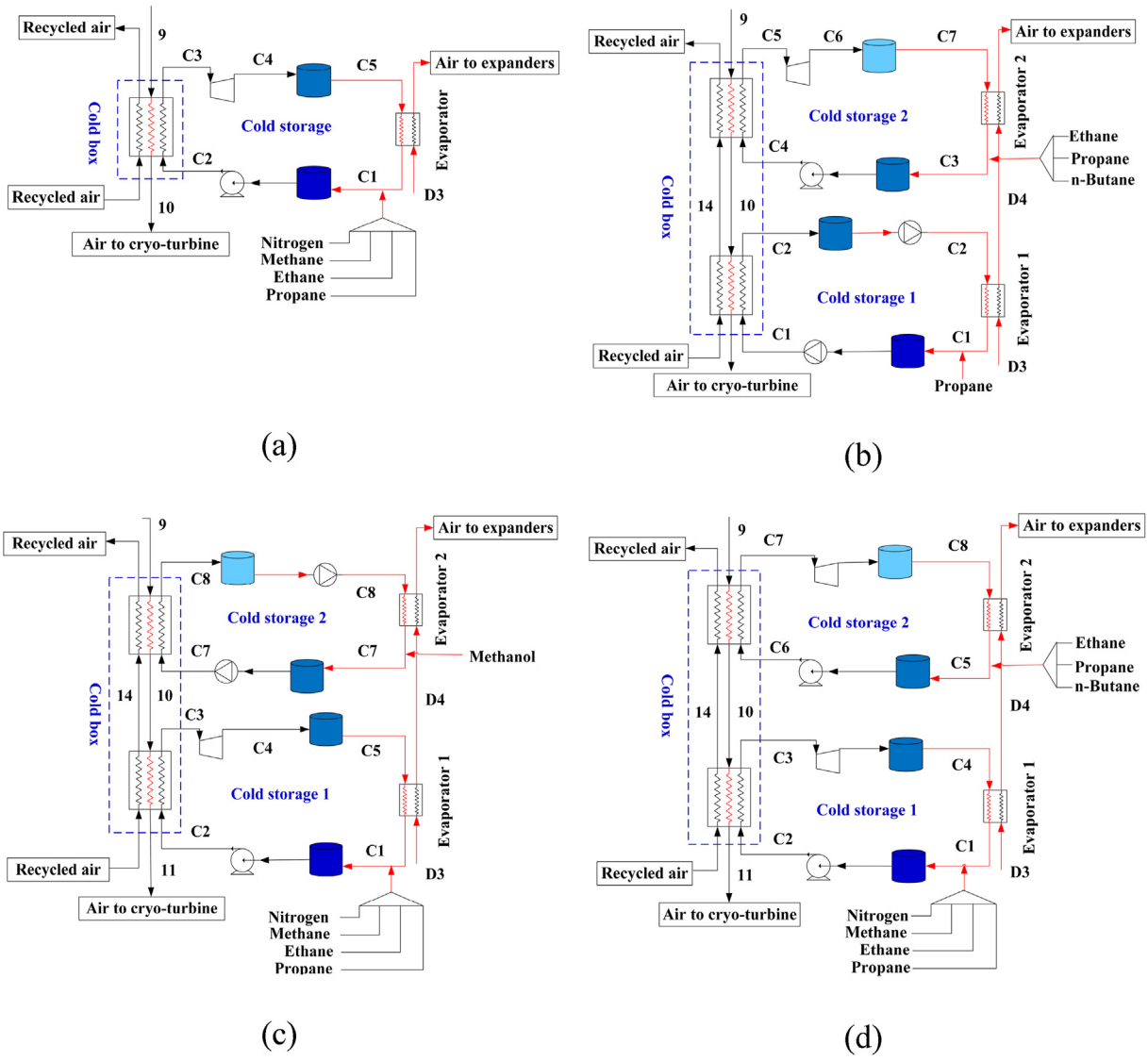

Fig. 4. Different configurations for cold energy storage cycles in the LAES: a) Case 3 (Single ORC); b) Case 4 (ORC + Propane cycle); c) Case 5 (Methanol cycle + ORC); d) Case 6 (Dual ORC).

$$\dot{W}_{net} = \sum \dot{W}_{comp} - \sum \dot{W}_{tur} \tag{4}$$

Here, $\dot{W}_{comp}$ and $\dot{W}_{tur}$ are the work of the compressors and turbines respectively.

In addition, exergy efficiency can be used to evaluate thermodynamic performance. While the LAES as a total system primarily deals with power, the charging and discharging parts, that operate at different times, handle both power and thermal energy (heating/cooling). Thus, it makes sense to use exergy that measures the quality of work and heat in a consistent way, considering both the first and second laws of thermodynamics. Without considering kinetic, potential, electrical, and nuclear exergies, the exergy of material streams includes physical (or thermo-mechanical) exergy and chemical exergy [25], see Equation (5).

$$\dot{E} = \dot{E}^{TM} + \dot{E}^{Ch} \tag{5}$$

Here, $\dot{E}^{TM}$ and $\dot{E}^{Ch}$ represent physical exergy and chemical exergy, respectively. Physical exergy is the maximum work obtained when the stream temperature and pressure is changed from its initial state to environment conditions by ideal (reversible) processes. Chemical exergy is the maximum work obtained when the stream is taken to a state that has the same composition as its natural surroundings, again by ideal (reversible) processes. Since no chemical reactions are present in the LAES system, chemical exergy has relatively small effects related to separation and mixing. As a consequence, only the physical exergy of streams is considered.

In this work, Exergy Transfer Effectiveness (*ETE*) is applied to measure the exergy efficiency of the LAES system. The *ETE* is defined as the exergy sinks (produced exergy) divided by the exergy sources (consumed exergy) in a process. The *ETE* considering only thermo-mechanical exergy was proposed by Marmolejo-Correa and Gundersen [26] and has been further developed by Kim and Gundersen [27] to include chemical exergy. The *ETE* with chemical exergy was successfully used as an objective function by Kim and Gundersen [28] to optimize LNG processes with NGL extraction. In those processes, similar to the LAES, there are no chemical reactions, but mixing and separation are more important, thus chemical exergy was also included.

The exergy efficiency can be expressed by using the definition of *ETE* as shown in Equation (6).

$$\eta_{\dot{E}} = ETE = \frac{\sum Exergy\ Sinks}{\sum Exergy\ Sources} \tag{6}$$

Actually, for energy storage systems, the charging process and the discharging process typically do not operate at the same time. Thus, the exergy efficiencies of these processes are considered separately to reveal the exergy transfer effectiveness within each process. The exergy efficiency of the charging process $\eta_{\dot{E}_{ch}}$ is calculated by Equation (7).

$$\eta_{\dot{E}_{ch}} = \frac{\dot{W}_{cryotur,ch} + \dot{E}_{liq} + \dot{E}_h}{\dot{W}_{comp,ch} + \dot{E}_c + \dot{E}_{fa}} \tag{7}$$

Here, $\dot{W}_{cryotur,ch}$ and $\dot{W}_{comp,ch}$ denote the expansion work produced by the cryo-turbine and the compression work consumed by compressors in the charging process. $\dot{E}_{liq}$, $\dot{E}_h$, $\dot{E}_c$ and $\dot{E}_{fa}$ represent the physical exergy of liquid air, working fluid in the hot storage cycle (thermal oil), working fluids in the cold energy storage cycles, and the air feed. The exergy of streams was calculated by embedding a Visual Basic code in an Aspen HYSYS flowsheet simulation as described by Abdollahi-Demneh et al. [29] and is based on the calculation methodology proposed by Kotas [25]. Similar to exergy efficiency for the charging process, the exergy efficiency of the discharging process $\eta_{\dot{E}_{dc}}$ is given by Equation (8).

$$\eta_{\dot{E}_{dc}} = \frac{\dot{W}_{tur,dc} + \dot{E}_c}{\dot{W}_{pump,dc} + \dot{E}_{liq} + \dot{E}_h} \tag{8}$$

Here, $\dot{W}_{tur,dc}$ and $\dot{W}_{pump,dc}$ are the expansion work produced by turbines and the work consumed by the pump in the discharging process, respectively.

4. Simulation, validation and optimization

The assumptions of the process model are provided in Section 4.1. The validation of the model and the optimization procedure for the LAES system are reported in Sections 4.2 and 4.3 respectively.

4.1. Process simulation

Simulation of the LAES system is conducted in Aspen HYSYS Version 10.0 [30]. The Peng-Robinson equation of state is adopted to calculate physical properties of the streams. Conditions of the air feed are provided in Table 2. In this work, the compression and expansion parts in the seven cases are the same, which means that a 4-stage compressor with inter-stage coolers in the compression section and a 4-stage turbine with reheaters in the expansion section are used in all cases. The multi-stream heat exchanger unit referred to as the LNG module in Aspen HYSYS is applied to model all heat exchangers in the system. Pressure drops and heat losses in heat exchangers, storage tanks and the flash tank are neglected in this work. Other simulation conditions and assumptions are shown in Table 3.

4.2. Model validation

The Aspen HYSYS model of the LAES has been validated against available data in the literature. Fig. 5 presents a comparison between this work and Guizzi et al. [12] of the LAES system performance. It is found that the differences between the values obtained using the simulation model in this work and the values in Guizzi's work are within 1.4%. Thus, a sufficient accuracy of the system model is confirmed, and the model is found to be acceptable for our research.

4.3. System optimization

The optimization model is implemented in Matlab, version R2018a [31]. The Particle Swarm Optimization (PSO) algorithm is applied to optimize the LAES system in this study. PSO is a population-based sampling optimization technique, and no global optimum can be guaranteed due to its stochastic nature. However, the advantage of using this algorithm is that no derivatives of mathematical equations are needed, thus it can be easily used in complex models such as this process [24]. The framework for the optimization is shown in Fig. 6. Moreover, the parameters for the PSO are listed in Table 4. The PSO algorithm is coded in Matlab and connected to Aspen HYSYS through the “actxserver” command. The motivation for the use of optimization is to make a fair comparison between the LAES system with different configurations and to find optimal compositions for multi-component working fluids for the corresponding cold energy recovery cycles. The objective is to maximize the round-trip efficiency of the LAES, as shown in Equation (9).

$$\min_x \ -\eta_{RT} = -f(x) = -\frac{\dot{m}_{liq} w_{tur}}{\dot{m}_{comp} w_{comp}} \tag{9}$$

The selection of decision variables, listed in Table 5 with their bounds and here represented by x, can be made by analyzing the degrees of freedom in the system. In this study, all pressure ratios for compressors and expanders are selected as variables. The outlet temperature of thermal oil from compression heat exchangers, the outlet air temperature from the cold box, and the outlet temperature of recycled air from the cold box are also selected as decision variables. In addition, operating temperatures, pressures and molar flowrates of working fluids are considered as variables. Variables for the LAES system with one or two cold energy recovery cycles are listed separately in Table 5, since the operating conditions of the two cycles are different.

The constraints for the LAES system are discussed in the following: The minimum temperature difference ($\Delta T_{\min}$) of

Table 2
Conditions of the air feed.

Conditions	Unit	Value
Air feed temperature	°C	20
Air feed pressure	bar	1
Air feed flow rate	kg/h	2000
Air feed composition		
Nitrogen	mole%	78.82
Oxygen	mole%	21.14
Argon	mole%	0.04

Table 3
Simulation conditions and assumptions.

Parameter	Value	Unit
Ambient temperature	20	°C
Ambient pressure	1	bar
Isentropic efficiency of compressor	85	%
Isentropic efficiency of gas turbine	90	%
Isentropic efficiency of cryo-turbine	75	%
Isentropic efficiency of pump	80	%

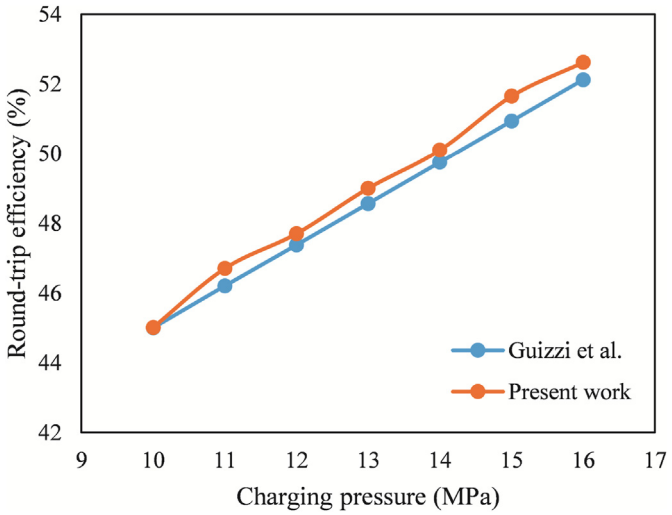

Fig. 5. Model validation by comparing RTE with numbers from Guizzi et al. [12].

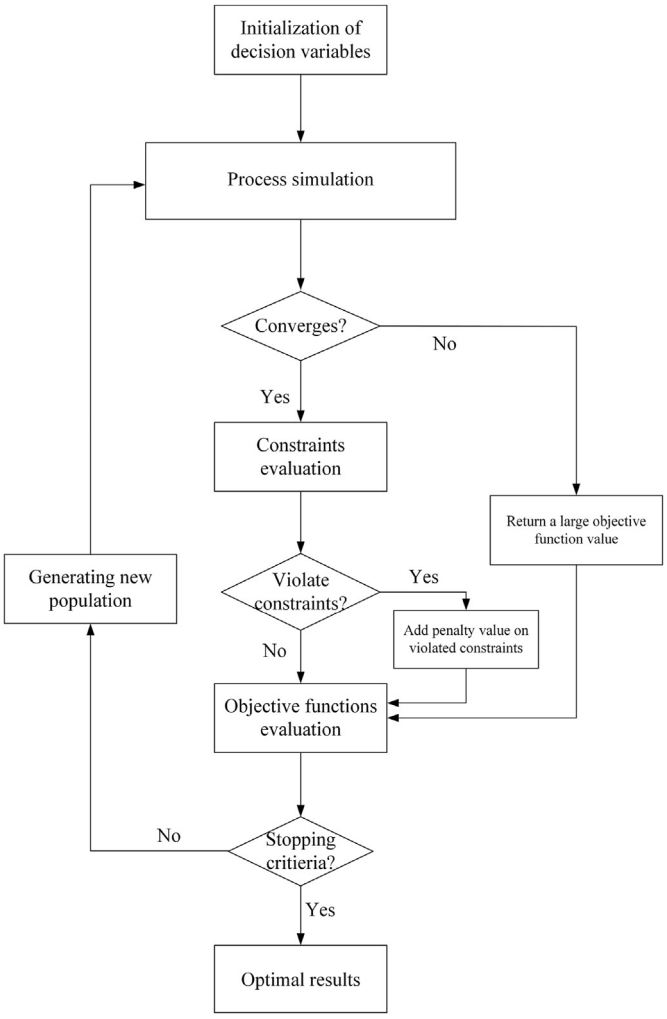

Fig. 6. Simulation-based optimization framework of the process.

intercoolers and reheaters is assumed to be 10 °C (see Equations (10) and (11)), while ΔT_{min} of the cold box and evaporators is assumed to be 1 °C (see Equations (12) and (13)), which is commonly used in low-temperature processes [32].

Table 4
Parameters of the PSO algorithm.

Parameters	Value
Number of particles	150
Cognition learning parameter	1.49
Social learning parameter	1.49
Maximum number of generations	500
Inertia weight coefficient	1

$$\Delta T_{int,ch} \geq 10 \quad (10)$$

$$\Delta T_{reh,dc} \geq 10 \quad (11)$$

$$\Delta T_{coldbox} \geq 1 \quad (12)$$

$$\Delta T_{eva} \geq 1 \quad (13)$$

In addition, for multi-component fluid cycles, the vapor fraction of the working fluid should be less than 0.005 to essentially assure liquid phase in the entire cycle, as shown in Equation (14). For ORCs, the vapor fraction of the working fluid at the inlet of the pump should be zero, indicating the phase to be totally liquid (see Equation (15)), and the vapor fraction of the working fluid at the outlet of the cold box (inlet stream to the turbine) should be one, indicating the phase to be totally gas (see Equation (16)).

$$VF_{MCFC} \leq 0.005 \quad (14)$$

$$VF_{ORC,pump,in} = 0 \quad (15)$$

$$VF_{ORC,tur,in} = 1 \quad (16)$$

5. Results and discussion

The optimal results of the seven cases are discussed here. The compression and expansion parts have the same configuration in all cases, i.e. four compressor stages and four expander stages. The difference between the seven cases is the cold energy recovery and storage part. Since optimization, however, is performed for the entire system, the compression and expansion parts are also included. As a result, the optimal operating conditions of the compression and expansion parts can be different for different cold energy recovery cycles. One example is that more compression work is needed to ensure sufficient refrigeration capacity for air liquefaction when the cold thermal energy recovery ratio is low.

5.1. RTEs for the seven cases

Fig. 7 illustrates the RTE for the LAES system with different cold energy recovery cycles. It shows that the LAES with two cold energy recovery cycles (Base Case and Cases 2, 4, 5 and 6) to transfer the cold regasification energy has better performance than the system with only one cold energy recovery cycle (Cases 1 and 3). The reason is that the temperature range for air is very large (from 30 °C to −180 °C) and the specific heat capacity of air changes significantly during the liquefaction and evaporation processes. Thus, better temperature match in the cold box can be obtained when two cold recovery fluids with different specific heat capacities are used. Among the five LAES configurations with two cold storage cycles, the LAES system with dual multi-component fluid cycle

Table 5
Decision variables with lower and upper bounds.

Variables	Lower Bounds	Upper Bounds
Pressure ratio for compressors[a,b]	1	5
Pressure ratio for expanders[a,b]	1	10
Thermal oil temperature ($T_{H21\text{-}H24}$) (°C)[a,b]	150	230
Cold box outlet air temperature (°C)[a,b]	−188	−165
Cold box outlet recycled air temperature (°C)[a,b]	−10	29
Working fluid operating temperature (higher) (°C)[a,b]	−10	29
Working fluid operating pressure (bar)[a,b]	1	120
Working fluid molar flowrate (kmol/h)[a,b]	0	60
Working fluid operating temperature (lower) (°C)[b]	−100	−20

[a] Variable bounds for the LAES with single cold cycle.
[b] Variable bounds for the LAES with dual cold cycle.

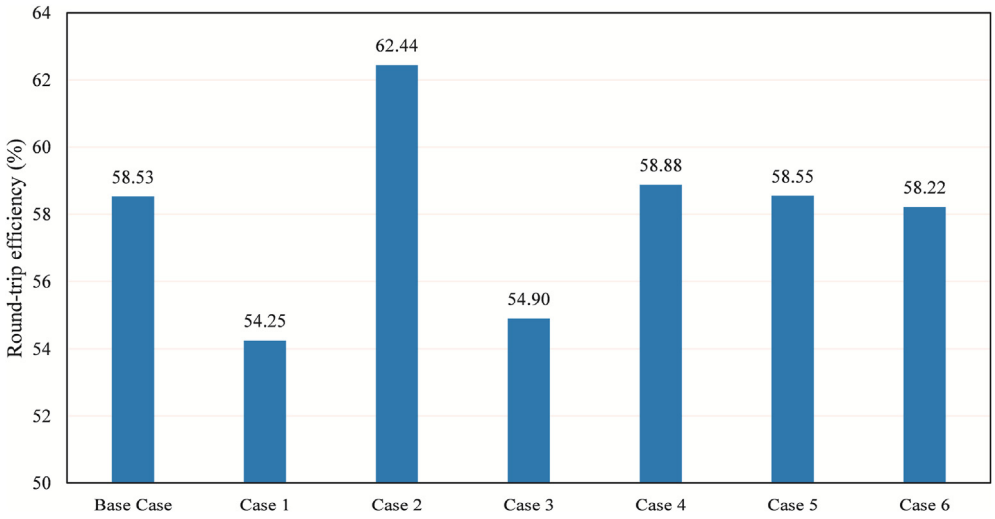

Fig. 7. Round-trip efficiency for the LAES system with different cold energy recovery cycles.

(MCFC) for cold thermal energy recovery has the highest RTE of 62.4%.

5.2. Optimal operating conditions for cold cycles

Optimal operating variables, such as temperatures, pressures and compositions for the working fluids are listed in Table 6 for the seven cases, while the optimal results (heat duty and logarithmic mean temperature difference (LMTD) of cold boxes) for different cold energy recovery cycles are shown in Table 7. In both tables, the terms 1st cycle and 2nd cycle refer to the cycle operating at higher and lower temperatures respectively.

Case 1. where only one MCFC is used rather than two single fluid cycles (methanol and propane cycles), is proposed to simplify the

Table 6
Optimal operating variables for different cold energy recovery cycles in the LAES system.

Cases	Cycle	Composition [mole%]						p [bar]	T_{lowest} [°C]	$p_{tur,in}$ [bar]	$p_{tur,out}$ [bar]
		CH_3OH	N_2	CH_4	C_2H_6	C_3H_8	nC_4H_{10}				
Base Case	1st	100.0	–	–	–	–	–	1.0	−46.7	–	–
	2nd	–	–	–	–	100.0	–	1.0	−186.3	–	–
Case 1	1st	–	0.1	10.8	7.5	81.6	–	85.8	−184.9	–	–
	2nd	–	–	–	–	–	–	–	–	–	–
Case 2	1st	–	–	0.3	4.1	47.4	48.2	32.2	−70.2	–	–
	2nd	–	3.0	2.8	18.6	75.6	–	27.4	−186.3	–	–
Case 3	1st	–	31.3	32.2	16.1	20.4	–	–	−186.5	4.9	4.9
	2nd	–		–	–	–	–	–	–	–	–
Case 4	1st	–	–	–	53.5	24.3	22.2	–	−43.6	6.9	6.8
	2nd	–	–	–	–	100.0	–	1.0	−184.1	–	–
Case 5	1st	100.0	–	–	–	–	–	1.0	−48.1	–	–
	2nd	–	21.0	39.8	18.3	20.9	–	–	−182.8	3.2	3.2
Case 6	1st	–	–	–	43.6	30.5	25.9	–	−40.1	4.5	4.5
	2nd	–	24.3	40.7	23.3	11.7	–	–	−188.0	3.2	3.2

Table 7
Optimal results for different cold energy recovery cycles in the LAES system.

Cases	Cycle	$Q_{coldbox}$	$LMTD_{coldbox}$	$LMTD_{eva}$	$\dot{m}_{ORC}$	$\dot{m}_F$
		[kW]	[°C]	[°C]	[kg/h]	[kg/h]
Base Case	1st	221.5	2.7	4.3	–	824.1
	2nd		2.8	3.9	–	2280.4
Case 1	1st	199.1	3.0	8.1	–	1733.5
	2nd		–	–	–	–
Case 2	1st	219.3	2.1	4.9	–	1221.3
	2nd		2.3	2.7	–	2402.9
Case 3	1st	203.5	4.4	6.7	968.6	–
	2nd		–	–	–	–
Case 4	1st	210.0	5.2	5.4	329.7	–
	2nd		2.1	5.8	–	2142.0
Case 5	1st	202.5	4.2	6.9	–	1022.1
	2nd		2.4	3.2	882.8	–
Case 6	1st	212.9	10.1	6.3	295.9	–
	2nd		3.3	4.4	859.4	–

configuration of the LAES system. In Case 2, the LMTDs for the cold box and evaporator are on average the smallest among the seven cases, indicating that the dual MCFC has the smallest entropy generation in the cold energy recovery part and thereby the highest thermodynamic efficiency. The operating pressures of the two MCFCs (p = 32.15 and 27.38 bar) in Case 2 are considerably reduced compared to the pressure of the single MCFC (p = 85.80 bar) in Case 1. This is due to the fact that working fluids experience a smaller temperature range in the cold boxes in Case 2 compared with Case 1, thus avoiding high pressure to keep the working fluids in liquid form.

It is worth noting that the operating pressures of the working fluids in Case 2 are considerably higher than the operating pressures in the Base Case (1 bar for both cycles). This, of course, increases the CAPEX of the system; however, the higher RTE of the LAES system with multi-component fluids will reduce OPEX. A trade-off analysis between CAPEX and OPEX will determine the economic feasibility of the system. In Case 2, the optimal composition of MCFC-1 is 0.26 mol% methane, 4.06 mol% ethane, 47.43 mol% propane and 48.25 mol% n-butane, while the optimal composition of MCFC-2 is 3.01 mol% nitrogen, 2.82 mol% methane, 18.56 mol% ethane and 75.61 mol% propane. The results show large fractions of propane and n-butane in the MCFCs, reflecting that these components have specific heat capacities closer to air. Methane and ethane are used to modify the composite curve of the working fluid for a better match with the air liquefaction curve. The amount of nitrogen is very small to keep the MCFC-2 working fluid in liquid form without the need for high pressure.

5.3. Using ORC as a cold energy recovery cycle

In Case 3, one ORC is used as the cold energy recovery cycle in the LAES system. The optimal results show that no power is produced in the ORC, because this single ORC operates without pressure change (the pump and turbine are inactive), which results in similar performance for Case 3 (single ORC) and Case 1 (single MCFC). The other four configurations (Base Case and Cases 4, 5 and 6) have similar RTEs, however, the optimal operating conditions are quite different. In the Base Case, methanol and propane cycles are used for cold energy recovery, and this configuration is discussed in many papers. The advantage of this configuration with an acceptable RTE of 58.5% is that the operating pressure of the two cold storage cycles is atmospheric, so that capital costs for cold storage tanks are reduced. For Case 4, the LAES with an ORC and a propane cycle has an RTE of 58.9%. The RTE of the LAES using methanol and an ORC as cold energy recovery cycles (Case 5) is 58.6%. It can be seen from Table 7 that the LMTDs for the cold boxes and evaporators in Cases 4 and 5 are similar, which is why the two cases have almost the same performance. In addition, the pressure ratios for turbines in the ORC in these cases are 1 ($p_{tur,in} = p_{tur,out}$), which indicates that running the ORC with power production is not optimal.

For the multi-component working fluid in the ORC, both the sensible and latent heat are used to collect the regasification energy of air. Since the ORC is able to collect more heat than the MCFC with sensible heat only, considerably less working fluid is needed for the ORC (see Table 7). The optimal composition of the working fluids can be found in Table 6, where ethane has the largest fraction in Case 4, accounting for 53.52 mol%, while the methane fraction (39.78 mol%) is the largest in Case 5. This is due to the fact that components with higher specific heat capacity, such as methane and ethane, are preferred when the mass flow rate of the working fluid is reduced. In Case 6, two ORCs act as heat transfer cycles, and both the sensible and latent heat of the working fluids are used to collect the cold thermal energy. The LMTDs of the cold boxes and evaporators are larger than the LMTDs in the Base Case and Cases 2, 4 and 5. As a result, the RTE of the LAES configuration with dual ORC is lower (58.2%) but still better than the RTEs of Cases 1 and 3. One conclusion from the optimal results of the different cases is that the operating pressure of the working fluid in the cold energy recovery cycles should be kept unchanged. This is because it is more efficient to use the cold energy collected from the regasification to liquefy air than producing work in the ORCs.

The driving forces between the liquefaction (charging) and regasification (discharging) curves for air in a T-H diagram are small. As shown in Fig. 8a, which is based on simulation results from Aspen HYSYS, the temperature of the working fluid is sometimes higher than the temperature of air in the cold box. However, this is not an indication of temperature cross-over in the heat exchanger. Recirculation air is also a cold fluid and contributes to the total heat capacity flowrate of the cold composite curve, and thereby avoids temperature cross-over in the cold box. Fig. 8b is an enlarged hand-drawn illustration of Fig. 8a. The gap between the air liquefaction or air regasification curves on one side and the evaporation or condensation curves of the working fluid in the ORC on the other side is artificially increased, i.e. drawn out of scale.

Results from the optimization indicate that the pressure ratio for the turbine and the pump in the ORC is 1, which means that the turbine and the pump are not active, and the ORC works like a multi-component fluid cycle (MCFC) with phase change. This also means that the composite curves in a T-H diagram for the working fluid in the cold box and the evaporator should coincide. However, with normal operation of the ORC (e.g. if the pressure ratio of the pump is 2), the specific enthalpy of the working fluid would be reduced, as the orange solid line shows in Fig. 8b. The match with the temperature profile of air would be less perfect in the evaporator, and the work produced by the ORC would not compensate for the lost work in the discharging part. The cold composite curve of air in the evaporator, i.e. the orange dotted line in Fig. 8b, is shifted down (the discharging pressure of liquid air is reduced to avoid temperature cross-over in the heat exchanger, since air at lower pressure has a higher heat of evaporation). Due to the work produced in the ORC when the pressure ratio is 2, the duty in the evaporator is reduced. This results in a lower air temperature after

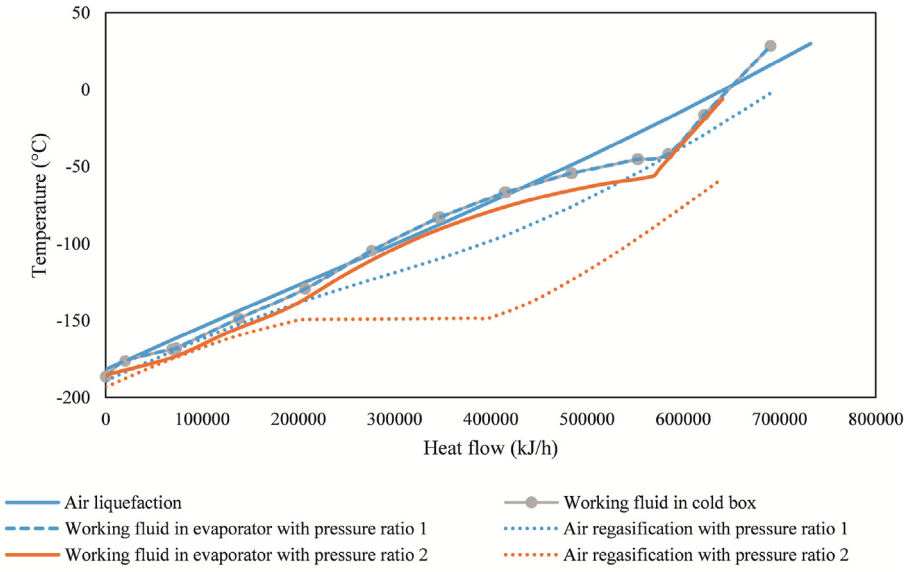

a)

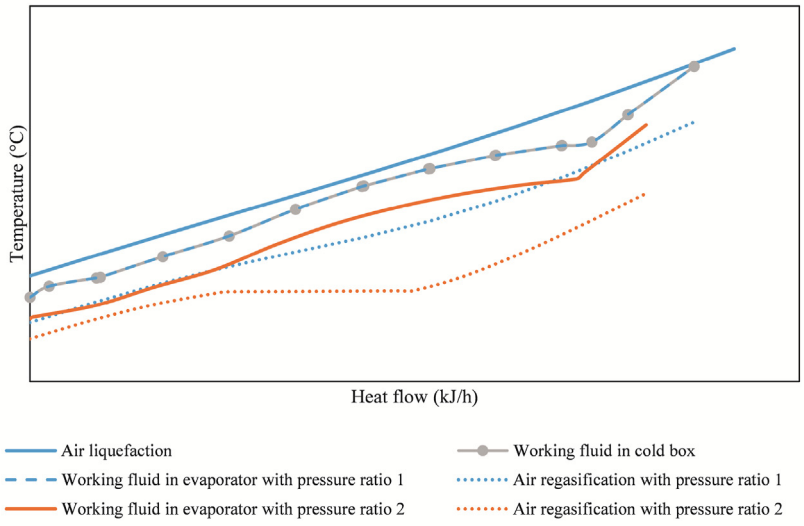

b)

Fig. 8. T-H diagram for the cold box and the evaporator in Case 3: a) Real data from Aspen HYSYS; b) Hand drawn figure to better explain the cold thermal energy transfer between the cold box and the evaporator.

the evaporator and therefore less work produced in the discharging part.

For Case 1, the sensible heat of the MCFC is used to transfer the cold duty from air regasification, and the change in the slope of the MCFC in the T-H diagram is relatively small compared to the change in the slope of air during the heat transfer process. Thus, poor performance (RTE = 54.3%) is the result due to the mismatch between the air and the single MCFC temperature profiles. The optimal composition of the single MCFC is shown in Table 6, where more than 80% is propane. Moreover, the operating pressure of the single MCFC is quite high (p = 85.80 bar), which leads to high capital costs. However, the situation is different for Case 3. An ORC with a multi-component working fluid is used for cold energy recovery. It can be seen from Table 6 that the pump and turbine are not active in this single ORC case, and the operating pressure (p = 4.87 bar) of the working fluid is reduced compared to Case 1. However, with the gradual evaporation and liquefaction of the working fluid, the temperature profiles between the air and the working fluid do not have a good match, which can be confirmed by the large LMTDs of the cold box and the evaporator ($LMTD_{coldbox}$ = 4.43 °C and $LMTD_{eva}$ = 6.72 °C). In this case, the optimal composition of the working fluid is 31.34 mol% nitrogen,

Table 8
Optimal results for some variables and key performance indicators.

	Base Case	Case 1	Case 2	Case 3	Case 4	Case 5	Case 6
p_{ch} (bar)	191.36	458.18	147.38	335.72	257.08	349.05	215.30
p_{dc} (bar)	145.38	175.94	100.62	109.26	150.02	186.30	108.59
η_{LY} (%)	86.65	88.54	93.79	91.55	91.09	91.61	92.42
SPC (kWh/t)	218.07	256.6	188.66	232.34	223.10	234.7	212.89
$\eta_{\dot{E}_{ch}}$ (%)	83.45	70.73	86.13	82.49	84.1	83.73	83.69
$\eta_{\dot{E}_{dc}}$ (%)	83.17	70.05	86.00	80.23	82.38	82.00	83.35
η_{RT} (%)	58.53	54.25	62.44	54.90	58.88	58.55	58.22

32.23 mol% methane, 16.08 mol% ethane and 20.35 mol% propane.

5.4. KPIs for the optimized cases

Table 8 shows optimal pressure values for charging and discharging together with key performance indicators (liquid yield, specific power consumption, exergy efficiencies of the charging and discharging processes, and round-trip efficiency) for the different cases. It can be seen that Case 2 has a superior performance compared to the other cases. Case 2 obtains the highest liquid yield (93.8%), highest exergy efficiencies of the charging (86.1%) and discharging (86.0%) processes, the smallest specific power consumption (188.66 kWh/t, which is consistent with the lowest charging pressure among the seven cases), and a superior round-trip efficiency (62.4%). These good results are primarily related to the best heat transfer efficiency of the dual MCFC. The difference in round-trip efficiency, exergy efficiency, liquid yield and specific power consumption is marginal for the Base Case and Cases 4, 5 and 6, except for the fact that the Base Case has a considerably lower liquid yield. The LAES with one cycle for cold recovery (Case 1) has the lowest RTE, which results from the mismatch between the air and working fluid temperature profiles. In Cases 1 and 3, higher charging pressures are needed to compensate for the reduced cold air regasification energy.

Fig. 9 illustrates exergy destructions for the compression, expansion and heat transfer parts in the seven cases. It can be noticed that Case 2 has the lowest exergy destruction in all three parts, while Cases 1 and 3 have the largest exergy destructions. The Base Case and Cases 4, 5 and 6 have medium exergy destructions. This is consistent with the previous discussion: Case 2 has the highest RTE, followed by the Base Case and Cases 4, 5 and 6, while Cases 1 and 3 have the lowest RTE. By comparing Cases 5 and 6, it is found that the total exergy destruction in Case 5 is higher. However, this mainly comes from the expansion part and is associated with larger work production, which improves the RTE. In addition,

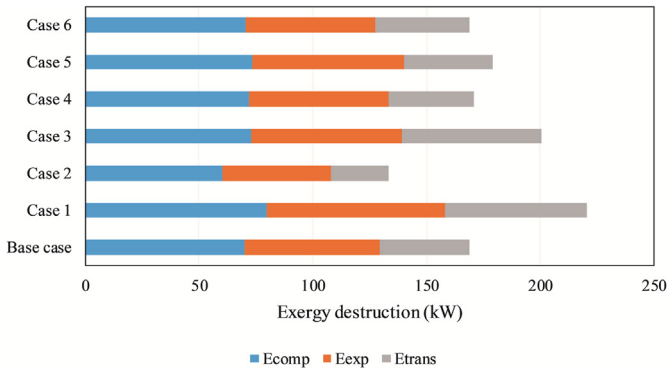

Fig. 9. Exergy destruction for the compression, expansion and heat transfer parts in the seven cases.

Table 9
Influence of cryo-turbine efficiency on system performance.

Cryo-turbine efficiency (%)	Optimal		η_{RT} (%)
	p_{ch} (bar)	p_{dc} (bar)	
65	149.23	95.71	61.29
75	147.38	100.62	62.44
85	143.71	101.55	63.12

exergy losses due to heat transfer are slightly smaller in Case 5. This reveals that the cold thermal energy transfer part, which is related to LMTDs of cold boxes and evaporators, and the liquid yield have decisive effects on the RTE of the system. Thus, higher efficiency of cold energy recovery cycles leads to a higher RTE.

6. Sensitivity analysis

The cryo-turbine efficiency and the ΔT_{min} of heat exchangers (high-temperature and low-temperature) have important influences on the system performance. As the LAES system with dual multi-component fluid cycles (Case 2) has the best performance according to Section 5, this process configuration is selected as the design basis for a sensitivity analysis. In Case 2, the isentropic efficiency of the cryo-turbine is 75%, and the ΔT_{min} of high-temperature and low-temperature heat exchangers are 10 °C and 1 °C, respectively. In this section, the cryo-turbine efficiencies of 65% and 85% are assumed and discussed. In addition, the ΔT_{min} of high-temperature heat exchangers are varied from 5 °C to 15 °C, and the ΔT_{min} of low-temperature heat exchangers is varied from 1 °C to 2 °C. The optimal results with different cryo-turbine efficiencies are listed in Table 9. For obvious reasons, the round-trip efficiency increases as the cryo-turbine efficiency is increased from 65 to 85%. It is worth noting that the optimal charging pressure is reduced with increasing cryo-turbine efficiency. Increased cryo-turbine efficiency results in a higher exergy efficiency of the equipment and a larger refrigeration capacity.

The influence of ΔT_{min} for heat exchangers is listed in Table 10. As the ΔT_{min} of high-temperature heat exchangers increases, exergy destructions for the compression and expansion parts are increased, while the exergy destruction for the heat transfer part remains almost the same. It should be emphasized that the compression part consists of compressors and intercoolers, the expansion part consists of expanders and reheaters, while the heat transfer part consists of the cold box, the evaporators, the cryo-turbine and the separator. Due to this decomposition, the heat transfer part is only affected by the ΔT_{min} for the low-temperature heat exchangers. Heat transfer in the high-temperature heat exchangers are accounted for in the compression and expansion parts. It is pointed out that the RTE is increased to 64.72% when the ΔT_{min} of high-temperature exchangers is dropped to 5 °C. However, the reduction of ΔT_{min} will result in a larger heat exchanger area and CAPEX, which is verified by the average *UA* values of high-temperature and low-temperature heat exchangers in Table 10. The *UA* value is the product of the overall heat transfer coefficient and heat transfer area, which can indicate the size of the heat exchanger. Thus, an economic analysis will be required to identify the cost optimal conditions for practical applications. In addition, the ΔT_{min} of the low-temperature heat exchangers affect the system performance significantly, since the liquid yield and the exergy destruction for the heat transfer part are related to this parameter. As the ΔT_{min} is increased to 2 °C in the low-temperature heat exchanger, a drop of 1.2% points for the RTE is observed. This mainly results from the increase in exergy destruction in the heat transfer part, as seen in Table 10.

Table 10
Influence of minimum approach temperature for heat exchangers on system performance.

Parameters	ΔT_{min} (°C)	$UA_{int/reh}$ (kW/°C)	$UA_{coldbox/eva}$ (kW/°C)	$\dot{E}_{comp}$ (kW)	$\dot{E}_{exp}$ (kW)	$\dot{E}_{trans}$ (kW)	η_{RT} (%)
High-temperature heat exchangers	5	11.51	44.87	56.89	32.91	24.39	64.72
	10	6.59	41.49	60.28	36.02	25.46	62.44
	15	4.03	40.16	68.66	41.66	25.32	58.56
Low-temperature heat exchangers	1	6.59	41.49	60.28	36.02	25.46	62.44
	2	6.58	29.35	61.50	36.63	30.00	61.22

7. Conclusions

The standalone liquid air energy storage (LAES) system with different cold energy recovery cycles is discussed, optimized and compared in this study. Multi-component fluid cycles (MCFCs) and Organic Rankine Cycles (ORCs) are considered for the first time to transfer the cold thermal energy from air regasification to air liquefaction in the LAES. Seven cases are optimized by using a particle swarm optimization (PSO) algorithm. For the different cold energy recovery cycles, the following conclusions are drawn:

- The dual MCFC has the best performance in terms of liquid yield, specific power consumption, exergy efficiency and round-trip efficiency (RTE). The RTE of the standalone LAES with dual MCFC in Case 2 is 62.4%. This RTE can, however, be improved to 64.7% when the ΔT_{min} of high-temperature heat exchangers is reduced from 10 °C to 5 °C. This performance is higher than standalone LAES systems in the literature with RTEs below 63%.
- Cases 1 and 3 with only one cold energy recovery cycle has lower RTE, since the specific heat capacity of the air is different before and after its phase change, and large exergy destructions are caused by the large temperature differences between the working fluid and air.
- Organic Rankine Cycles are not suitable for transferring the cold duty between the charging and discharging processes. The optimal results show that both the sensible and latent heat of the working fluid are used, however, the pump and turbine are not active. The purpose of using an ORC (i.e. to produce additional work) is therefore not achieved. The actual heat transfer is between the air regasification and air liquefaction, and a better match can be obtained in both cold boxes and evaporators when the operating temperature and pressure of the working fluid is kept the same on both sides.

The scope of this study has been limited to considering different configurations of cold energy recovery cycles in order to improve LAES systems. Future research can be divided into two distinct areas:

(1) The RTE of stand-alone LAES systems can be improved in several ways. There is waste heat in the hot oil cycle transferring heat from the compression section to the expansion section. The best cold energy recovery system identified in this work with two MCFCs has the disadvantage of relatively high operating pressure to ensure the working fluids are in liquid phase throughout the cycles. This has a negative effect on capital cost, and search for alternative chemical components in the working fluids should be conducted. Since there is an obvious trade-off between capital cost and RTE, cost analysis of the dual MCFC system should be performed in order to evaluate the economic feasibility of an LAES with this level of complexity.

(2) Integration of the LAES system with available heat sources (such as waste process heat) and/or heat sinks (such as regasification of LNG) at appropriate temperatures could also improve the RTE of the LAES considerably.

Credit authors statement

Zhongxuan Liu is the first author and main researcher behind the manuscript. She has developed the ideas, built the simulation models and conducted the optimizations: Donghoi Kim has been a discussion partner, in particular on the simulation models and the organization of the optimization: Truls Gundersen as the corresponding author has been responsible for the quality of the language and the structure as well as the layout of the manuscript.

Declaration of competing interest

The authors declare that they have no known competing financial interests or personal relationships that could have appeared to influence the work reported in this paper.

Acknowledgements

This publication has been funded by HighEFF - Centre for an Energy-Efficient and Competitive Industry for the Future. The authors gratefully acknowledge the financial support from the Research Council of Norway and user partners of HighEFF, an 8-years Research Centre under the FME-scheme (Centre for Environment-friendly Energy Research, 257632).

Nomenclature

Symbols

A	Heat exchanger area (m^2)
$\dot{m}$	Mass flow rate (kg/s)
$\dot{E}$	Exergy (kW)
p	Pressure (bar)
T	Temperature (°C)
VF	Vapor fraction
η	Efficiency (%)
ΔT	Minimum heat transfer approach temperature (°C)
U	Overall heat exchanger coefficient ($kW/°C \cdot m^2$)
$\dot{W}$	Power (kW)
w	x Specific power (kJ/kg) Set of decision variables

Subscripts

c	Cold fluids (working fluids in cold storage cycles)
ch	Charging process
$cryotur$	Cryo-turbine
$coldbox$	Cold box

dc	Discharging process
comp	Compression/Compressor
eva	Evaporation/Evaporator
F	Fluid
fa	Air feed
h	Hot oil (working fluid in the hot storage cycle)
in	Inlet
int	Intercooler
liq	Liquid air
LY	Liquid yield
net	Net power output
out	Outlet
pump	Pump
reh	Reheater
RT	Round-trip efficiency
trans	Heat transfer part
tur	Turbine

Acronyms

CAES	Compressed Air Energy Storage
DES	Distributed Energy System
EES	Electrical Energy Storage
LAES	Liquid Air Energy Storage
LMTD	Logarithmic Mean Temperature Difference
LNG	Liquefied Natural Gas
MCFC	Multi-component Fluid Cycle
NPP	Nuclear Power Plant
ORC	Organic Rankine Cycle
PHES	Pump Hydroelectrical Energy Storage
PSO	Particle Swarm Optimization
RTE	Round-Trip Efficiency

References

[1] British Petroleum. BP statistical review of world energy report. London, UK: BP; 2019.
[2] British Petroleum. BP energy outlook. London, UK: BP; 2020.
[3] Rozali NEM, Wan Alwi SR, Manan ZA, Klemeš JJ, Hassan MY. Optimisation of pumped-hydro storage system for hybrid power system using power pinch analysis. Chem Eng Trans 2013;35:85–90.
[4] Alanne K, Saari A. Distributed energy generation and sustainable development. Renew Sustain Energy Rev 2006;10(6):539–58.
[5] Aneke M, Wang M. Energy storage technologies and real life applications–A state of the art review. Appl Energy 2016;179:350–77.
[6] Rehman S, Al-Hadhrami LM, Alam MM. Pumped hydro energy storage system: a technological review. Renew Sustain Energy Rev 2015;44:586–98.
[7] Bullough C, Gatzen C, Jakiel C, Koller M, Nowi A, Zunft S. Advanced adiabatic compressed air energy storage for the integration of wind energy. In: Proceedings of the European wind energy conference; 2004. London, UK.
[8] Gallo AB, Simões-Moreira JR, Costa HKM, Santos MM, Moutinho dos Santos E. Energy storage in the energy transition context: a technology review. Renew Sustain Energy Rev 2016;65:800–22.
[9] Damak C, Leducq D, Hoang HM, Negro D, Delahaye A. Liquid air energy storage (LAES) as a large-scale storage technology for renewable energy integration – a review of investigation studies and near perspectives of LAES. Int J Refrig 2020;110:208–18.
[10] Smith EM. Storage of electrical energy using supercritical liquid air. Proc Inst Mech Eng 1977;191(1):289–98.
[11] Highview power. 2019. Benefits, www.highviewpower.com/technology/. [Accessed 29 May 2020].
[12] Guizzi GL, Manno M, Tolomei LM, Vitali RM. Thermodynamic analysis of a liquid air energy storage system. Energy 2015;93:1639–47.
[13] Morgan R, Nelmes S, Gibson E, Brett G. An analysis of a large-scale liquid air energy storage system. Proc Institution Civil Eng Energy 2015;168(2):135–44.
[14] Borri E, Tafone A, Romagnoli A, Comodi G. A preliminary study on the optimal configuration and operating range of a “microgrid scale” air liquefaction plant for Liquid Air Energy Storage. Energy Convers Manag 2017;143:275–85.
[15] Liu Z, Yu H, Gundersen T. Optimization of liquid air energy storage (LAES) using a genetic algorithm (GA). Computer Aided Chem Eng 2020;48:967–72.
[16] Chen J, An B, Yang L, Wang J, Hu J. Construction and optimization of the cold storage process based on phase change materials used for liquid air energy storage system. J Energy Storage 2021;41:102873.
[17] Peng X, She X, Cong L, Zhang T, Li C, Li Y, et al. Thermodynamic study on the effect of cold and heat recovery on performance of liquid air energy storage. Appl Energy 2018;221:86–99.
[18] Li Y, Cao H, Wang S, Jin Y, Li D, Wang X, et al. Load shifting of nuclear power plants using cryogenic energy storage technology. Appl Energy 2014;113:1710–6.
[19] Cetin TH, Kanoglu M, Yanikomer N. Cryogenic energy storage powered by geothermal energy. Geothermics 2019;77:34–40.
[20] Lee I, Park J, Moon I. Conceptual design and exergy analysis of combined cryogenic energy storage and LNG regasification processes: cold and power integration. Energy 2017;140:106–15.
[21] Lee I, You F. Systems design and analysis of liquid air energy storage from liquefied natural gas cold energy. Appl Energy 2019;242:168–80.
[22] Qi M, Park J, Kim J, Lee I, Moon I. Advanced integration of LNG regasification power plant with liquid air energy storage: enhancements inflexibility, safety, and power generation. Appl Energy 2020;269:115049.
[23] Antonelli M, Barsali S, Desideri U, Giglioli R, Paganucci F, Pasini G. Liquid air energy storage: potential and challenges of hybrid power plants. Appl Energy 2017;194:522–9.
[24] Eberhart R, Kennedy J. A new optimizer using particle swarm theory. Proc Sixth Int Symposium Micro Machine Human Sci 1995:39–43.
[25] Kotas TJ. The exergy method of thermal plant analysis. London, UK: Exergon Publishing Company with Paragon Publishing.; 2012.
[26] Marmolejo-Correa D, Gundersen T. A new efficiency parameter for exergy analysis in low temperature processes. Int J Exergy 2015;17(2):135–70.
[27] Kim D, Gundersen T. Development and use of exergy efficiency for complex cryogenic processes. Energy Convers Manag 2018;171:890–902.
[28] Kim D, Gundersen T. Use of exergy efficiency for the optimization of LNG processes with NGL extraction. Energy 2020;197:117232.
[29] Abdollahi-Demneh F, Moosavian MA, Omidkhah MR, Bahmanyar H. Calculating exergy in flowsheeting simulators: a HYSYS implementation. Energy 2011;36(8):5320–7.
[30] HYSYS A. Version 10.0. Burlington, Massachusetts: Aspen Technology Inc.; 2017.
[31] MATLAB. 9.4.0.813654 (R2018a). Natick, Massachusetts: The MathWorks Inc.; 2018.
[32] Higginbotham P, White V, Fogash K, Guvelioglu G. Oxygen supply for oxyfuel CO2 capture. Int J Greenhouse Gas Control 2011;5:S194–203.